Int. J. Exp. Path. (2004), 85, 85–96

ORIGINAL ARTICLE

Cathepsin L-deficient mice exhibit abnormal skin and bone development and show increased resistance to osteoporosis following ovariectomy

Wendy Potts[*], Jonathan Bowyer[*], Huw Jones[*], David Tucker[*], Anthony J. Freemont[†], Andrew Millest[*], Colin Martin[*], Wendy Vernon[*], Diane Neerunjun[*], Gillian Slynn[*], Fiona Harper[*] and Rose Maciewicz[*]

[*]*AstraZeneca Pharmaceuticals, Cheshire, UK, and* [†]*Department of Rheumatology, University of Manchester, Manchester, UK*

INTERNATIONAL JOURNAL OF EXPERIMENTAL PATHOLOGY

Summary

The role of cathepsin L in normal physiological processes was assessed using cathepsin L homozygous knockout mice (B6;129-Ctsl^{tm1Alpk}). These mice were generated using gene targeting in embryonic stem cells. Null mice fail to express mRNA and protein to cathepsin L. They developed normally and were fertile. The distinct phenotypic change exhibited was a progressive hair loss, culminating in extensive alopecia by 9 months of age. Histological analysis of the skin from homozygous mice revealed diffuse epithelial hyperplasia, hypotrichosis, hair shaft fragmentation and utricle formation. These findings provide evidence that cathepsin L is involved in the regulation of epithelial cell proliferation and differentiation in the skin. In addition, the role of cathepsin L in bone remodelling was evaluated. Using bone histomorphometric measurements, trabecular, but not cortical, bone volume was found to be significantly decreased in the cathepsin L heterozygote and homozygote mice compared to the wild-type mice. Following ovariectomy, it was observed that loss of trabecular bone, the most metabolically active component of bone, occurred to a lesser extent in homozygote, and heterozygote mice, than was seen in wild-type mice. These observations suggest that cathepsin L is likely to have a role in controlling bone turnover during normal development and in pathological states.

Keywords
cathepsin L, knockout mice, osteoporosis, ovariectomy

Received for publication 28 January 2003
Accepted for publication 28 January 2004

Correspondence:
David Tucker
AstraZeneca Pharmaceuticals
Alderley Park
Mereside, Macclesfield
Cheshire SK10 4TG, UK
Fax: +44 1625 510061
E-mail: david.tucker@astrazeneca.com

Cathepsin L is a ubiquitously expressed proteinase belonging to the papain family of cysteine proteinases that include the related cathepsins B, L, H, K, S, F and W. Its intralysosomal location and ability to degrade a broad spectrum of proteins suggest that it may play a role in general protein turnover (Everts *et al*. 1996) and/or antigen presentation and processing (Katunuma *et al*. 1998; Nakagawa *et al*. 1998). However, cathepsin L is also known to be secreted, and because it has been shown to degrade many extracellular matrix proteins, including the bone type I collagen (Kirschke *et al*. 1982),

basement membrane type IV collagen (Maciewicz *et al.* 1989) and the cartilage collagens II, IX and XI (Maciewicz *et al.* 1990), it has been hypothesized to play a role in osteoporosis, cancer and arthritis.

Gene knockout mice play an important role in assessing the functional analysis of mammalian genes. Within the papain family of cysteine proteinases, knockouts of cathepsins B, K, S and L have been generated. All of these knockouts appeared to undergo normal development and were fertile, suggesting that there is redundancy of these genes in the papain family. While cathepsin K knockouts display an osteopetrotic phenotype with excessive trabeculation of the bone-marrow space (Saftig *et al.* 1998, 2000), and cathepsin L knockouts show progressive alopecia (Roth *et al.* 2000), a detailed analysis of other cysteine proteinase knockouts has been required to identify more selective roles for the other proteinases in this family. This has been exemplified in the study of antigen presentation where different antigen presenting cells (APCs) use distinct proteinases to mediate major histocompatibility complex (MHC) class II maturation and peptide loading. Knockouts have shown that cathepsin L appears to have a critical role in the degradation of invariant chain in cortical thymic epithelial cells but not in bone-marrow-derived APCs (Nakagawa *et al.* 1998). While the ability to degrade invariant chain in professional APCs (splenocytes and dendritic cells) appears to be under the control of cathepsin S (Nakagawa *et al.* 1999; Shi *et al.* 1999), studies of the double knockout of cathepsins S and L have highlighted a third cysteine proteinase, cathepsin F, to be involved in invariant chain cleavage in macrophages (Shi *et al.* 2000). Moreover, cathepsin B does not appear to be essential for MHC class II-mediated antigen presentation, as degradation of invariant chain proceeded normally in cath $B^{-/-}$ splenocytes (Deussing *et al.* 1998).

Knowledge of the role of cysteine proteinases in disease can be strengthened by study of the effects of the knockout on the characteristics of disease models in animals. For instance, cathepsin S knockouts have been shown to have a diminished susceptibility to collagen-induced arthritis (Nakagawa *et al.* 1999), while cathepsin B plays a role in intrapancreatic trypsinogen activation and the onset of acute pancreatis (Halangk *et al.* 2000).

In the current report, we describe major phenotypic changes associated with hair growth and skin differentiation as well as trabecular bone quantity in cathepsin L null mice. In addition, because cathepsin L has been proposed to have a role in bone remodelling, the effects of its disruption were investigated in an oestrogen-deficiency model of osteoporosis in ovariectomized mice.

Materials and methods

Cloning of the murine cathepsin L gene and construction of a targeting vector

A lambda 129/Sv mouse genomic library (Stratagene, La Jolla, CA, USA) was screened using a full-length murine cathepsin L cDNA as a probe. The gene targeting backbone vector pPGK-Neo was constructed by subcloning a Pgk-neo expression cassette from plasmid pKJ1 (Adra *et al.* 1987; Tybulewicz *et al.* 1991), into the *Sma*I site of pBluescript. The *neo* gene is under the control of the mouse *phosphoglycerate kinase 1* (*Pgk-1*) gene promoter with 3′ termination sequences from Pgk-1. A 1.2 kb genomic fragment spanning part of cathepsin L exon 2 through to the start of exon 4 was polymerase chain reaction (PCR) amplified with *Not*I ends from the cathepsin L genomic clone. This fragment was subcloned into the *Not*I site, upstream of PGK-Neo. A 3.8 kb *Eco*RI fragment from exon 4 was subcloned downstream of the PGK-neo cassette. The neo cassette transcribes in the opposite direction to the cathepsin L gene and is located upstream of the active site of the enzyme. The final plasmid construct was linearized by *Sal*I digestion prior to transfection.

Generation of ES cell clones with cathepsin L-targeted integration

HM-1 ES cells, derived from mouse strain 129P2/Ola, were electroporated with linearized vector and were cultured in the presence of Leukemia Inhibitory Factor (LIF) (1000 U/ml) without a feeder layer of 3T3 cells. Selection with G418 (350 mg/ml) was applied after 24 h. Clones were isolated for analysis and expansion on days 10–12 according to the method of McPheat *et al.* (1991). Genomic DNA from clones was analysed by PCR to identify targeted recombinants. PCR primers were designed such that the forward primer anneals to sequence flanking the target and the reverse primer anneals to the PGK-neo sequence in the incoming DNA. A PCR product of predetermined size is produced only following homologous recombination. Genomic DNA from clones was digested with *Bgl*I and analysed further by Southern blotting using an external probe. This hybridizes to part of exon 8 in the 3′ region flanking the targeting vector, giving rise to a 5.8 kb wild-type fragment.

Generation of cathepsin L-deficient mice

C57BL/6Alpk (BL/6) blastocysts were microinjected with embryonic stem cells from two targeted recombinant clones to generate cathepsin L-deficient mice. Outbred mice with a

mixed genetic background comprising BL/6 × 129/OlaHsd were analysed in study 1. Homozygous mice from study 1 were backcrossed for five generations to BL/6 mice to produce partially inbred mice for study 2 and to 129/OlaHsd (129) mice for five generations to yield partially inbred mice for study 3. All animal procedures were carried out in compliance with the U.K. Animals (scientific procedures) Act 1986 and associated Home Office guidelines.

Genotyping of mice

Genomic DNA was prepared from mouse tissue samples according to the protocol of Laird *et al.* (1991). DNA was digested with either *Bgl*I or *Xho*I and probed with a cDNA probe spanning exons 2–6. *Bgl*I fragment sizes were as previously described. Following *Xho*I digestion, fragment sizes were 2.0 kb for wild-type and 4.0 kb for the targeted allele.

Skin histology

Histological analysis of skin was undertaken on cathepsin L homozygote and wild-type mice (BL/6 × 129) at 3 months and 9 months of age. Homozygote and wild-type mice from backcrossing onto a 129/Ola background were analysed at 4 months of age. Two adjacent samples of interscapular skin, cut in the longitudinal plane, were taken from the dorsal midline of each mouse after culling with a rising concentration of carbon dioxide. Tissues were fixed by immersion in 10% neutral phosphate-buffered formalin, processed into paraffin wax and 5-μm-thick sections were stained with haematoxylin and eosin and examined by light microscopy.

Biochemical analysis of cathepsin L and B in mouse tissues

Samples of spleen, kidney and liver were excised from wild-type, cathepsin L heterozygote and homozygote mice. The tissues were weighed and homogenized, in two times the tissue volume of 50 mM sodium acetate (pH 5.0), 1 mM Na_2EDTA and 0.25% (w/v) Triton-X100 using a polytron. The homogenates were then extracted for 1 h at 4 °C, after which they were centrifuged at 15 000 × ***g*** for 20 min. These samples were separated on an isoelectric focusing (IEF) gel, and cathepsin L and B activity was detected using the synthetic substrate Z-Phe-Arg-NMec (10 μM, Sigma) overlay, in the absence or presence of a specific inhibitor of cathepsin B (10 μM Ca074, Sigma). Human cathepsin L, purified from liver as described previously (Maciewicz *et al.* 1990), was used as a standard on the IEF gel.

Agarose isoelectric focusing

An agarose IEF (Pharmacia, New York, NY, USA) gel was cast onto a hydrophilic polyester sheet (GelBond^{TM}) following manufacturer's instructions. Equal amounts of Ampholine (pH 5–7 and pH 3.5–9.5) (Pharmacia) were used to create a pH gradient of pH 4–9. The samples were separated, and activity was detected as described previously (Maciewicz & Etherington 1988).

Ovariectomy

Ovariectomy or sham (SHAM) surgery was carried out on female wild-type, cathepsin L heterozygote and homozygote mice aged approximately 3 months. Mice were anaesthetized using an intraperitoneal injection of fentanyl/midazolam. Using aseptic techniques, the ovaries were exposed via a single midline dorsal incision and either removed by blunt dissection (ovariectomy) or replaced in the peritoneal cavity (SHAM), and the skin wound was closed with clips. Following ovariectomy, the mice were housed with free access to food and water. The animals were humanely killed 6 weeks after surgery, and bone and tissue samples were removed for analysis.

Analysis of bone

The left and right femurs were excised from wild-type, cathepsin L heterozygote and homozygote mice that had undergone ovariectomy or SHAM surgery. The bones were stripped clean of all soft tissue, and the ash mineral weight of the left femurs was determined after overnight ashing at 1100 °C.

The right femurs were sent to the laboratory in neutral buffered formalin and hemisected transversely through the shaft. The tissue was then processed, stained and examined using the routine techniques employed for human bone histomorphometry (Lalor *et al.* 1986; Haworth *et al.* 2000). Briefly, the lower ends of the femurs were fixed in absolute alcohol for 7 days before embedding in LR white resin (London Resin Company, Reading, Berkshire, UK) using an automated 7-day cycle during which gradual substitution of the alcohol by monomer was performed. The resin was then polymerized in an anoxic atmosphere, and the block was cut with a diamond saw, such that the cut surface of the block was parallel to the long axis of the femur and the bone was cut in the coronal plane. Each block was transferred to a powered microtome, and the block was trimmed to a point where the cruciate ligaments first appeared at the surface.

Ten 7 μm step serial sections were taken from the block (one every 50 μm), and alternate sections were stained with toluidine blue and von Kossa's stain. Each section was placed on the stage of a Leitz MB45 microscope, and the image was captured using a Quantimet 600 image analyser. Measurements of length, area and distance were made following the protocol recommended by the American Society for Bone and Mineral Research (Parfitt *et al*. 1987), and these were converted automatically to cortical and trabecular bone volumes by the image analysis software.

Statistical analysis

All data are expressed as mean ± standard deviation. Statistical differences between the groups were evaluated using two-sided, unequal variance Student's *t*-test. *P*-Values less than 0.05 were considered to be significant.

Results

Generation of mice with a mutated cathepsin L gene

The cathepsin L mutant mice were generated by homologous recombination in HM-1 ES cells. A neomycin phosphotransferase expression cassette was inserted into the *Eco*RI site of exon 4 by gene targeting in embryonic stem cells (Figure 1a). The construct was designed such that there was 1.2 kb of flanking homology in the 5′ region and 3.8 kb of homologous sequence at the 3′ end. Nine putative positive clones containing a targeted integration were identified initially by PCR using a forward primer in the region flanking the integration site and a reverse primer in the neo expression cassette. Gene targeting was confirmed by Southern analysis with a partial exon 8 external probe and an internal probe comprising exons 2–6 of the cathepsin L cDNA. Integration of the neo cassette into the cathepsin L gene leads to the introduction of a *Bgl*I site into a 5.8 kb wild-type *Bgl*I fragment. This results in the appearance of a 4.0 kb targeted fragment with the external probe (Figure 1b). Hybridization with the internal probe revealed the 3.8 and 4.0 kb bands, characteristic of gene targeting (Figure 1c).

Three targeted ES cell clones were selected for microinjection into blastocysts from strain BL/6. Resulting chimeras were backcrossed with BL/6 mice. Two of the three clones were transmitted through the germline to yield heterozygous (cathepsin L+/–) mice, identified by Southern hybridization. Heterozygotes were intercrossed, and genotypes of progeny were determined by Southern hybridization (Figure 1b). The homozygote, heterozygote and wild-type offspring that were produced conformed to the expected ratios from heterozygote intercrosses.

Northern blot analysis of mRNA from liver and brain tissue revealed a complete absence of signal for cathepsin L in mice homozygous for the gene disruption (data not shown). Cathepsin L enzymatic activity, in liver homogenates of wild-type, cathepsin L heterozygote and homozygote mice, was analysed using IEF and the synthetic substrate Z-Phe-Arg-NHMec in the absence (Figure 1d) and presence of the cathepsin B-specific inhibitor Ca074 (Figure 1e). The data indicated that although cathepsin L activity was observed in wild-type and heterozygote mice, no cathepsin L activity could be detected in homozygote mice. In addition, cathepsin B levels were not upregulated in homozygote cathepsin L mice. Similar results were found for spleen and kidneys (data not shown).

Cathepsin L knockout mice display skin and hair abnormalities

Homozygote mice could be readily distinguished from their heterozygote, and wild-type littermates, by the appearance of their coats at weaning and beyond (Figure 2). This phenotype was characterized by reduced hair length and a reduction in density. The normal sleek, smooth coat patina was replaced by a dull greasy appearance. These features were sufficiently distinctive at weaning to reliably identify the young homozygous mice and developed into extensive hair loss by 9 months of age (Figure 2a–c). Mice derived from both targeted clones exhibited this phenotype. At weaning, heterozygote and wild-type young were phenotypically normal and visually indistinguishable from each other, but by 9 months, there were differences between these mice (Figure 2c). Mice of all genotypes were fertile and bred normally.

At approximately 3 months of age, the BL/6 × 129 homozygous male and female cathepsin L mice developed progressive hair loss, which originated dorsally and gradually extended over the entire surface of the animal by 9 months of age. This effect was more profound in females, such that by 9 months of age, the female homozygotes showed total hair loss (Figure 2b), whereas the males retained patchy areas of sparse hair (Figure 2c). Vibrissae were present in both sexes but were sparse and attenuated in comparison with normal littermates. There was no regeneration of hair as the mice aged beyond 9 months. Heterozygote offspring also developed hair loss but later than the homozygote mice. At 9 months, the heterozygote cathepsin L females had a bald area covering the central dorsal surface (Figure 2b), but the males showed only small patches of baldness, which were randomly distributed over the dorsal surface (Figure 2c). All wild-type offspring had normal coat and vibrissae formation (Figure 2a–c).

The onset of hair loss occurred earlier in those mice obtained from backcrossing the null mutation for five generations to the inbred strain, BL/6. In these animals, hair loss

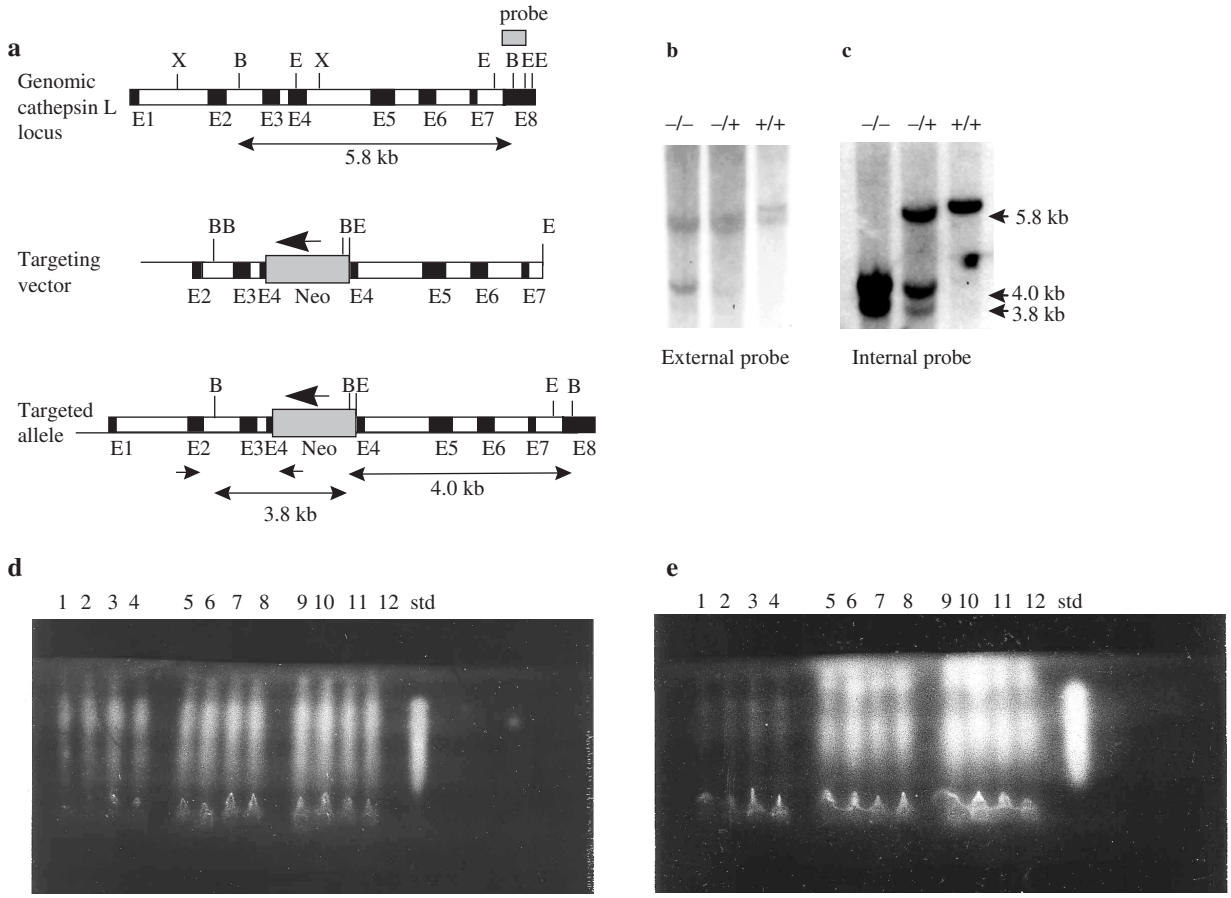

Figure 1 Targeted disruption of the cathepsin L gene locus. (a) Homologous recombination at the cathepsin L gene locus. The structural organization of the cathepsin L gene is represented by the top line. Exons are shown by filled boxes designated E1–E8. The middle line shows the targeting vector containing a neo expression cassette inserted into exon 4. The neo is transcribed in the opposite orientation to the cathepsin L gene, shown by the large arrow. The lower line shows the predicted structure of the locus following targeted integration. Positions of polymerase chain reaction (PCR) primers used in the primary screen are indicated by small arrows. The *5´* primer is in the region flanking the targeting vector. The external Southern probe hybridizing to part of exon 8 is shown as a dark box. Restriction sites: B (*Bgl*I); E (*Eco*RI); X (*Xho*I). Exon sizes are not to scale. (b) Genomic Southern blot of DNA from homozygote knockout (–/–), heterozygote knockout (+/–) and wild-type (+/+) mice, digested with *Bgl*I and probed with the external exon 8 probe are shown. (c) Genomic Southern blot from panel b, stripped and re-probed with an internal cDNA probe spanning exons 2–6. Fragment sizes for both panels b and c are shown to the right. (d) Analysis of cathepsin L and B levels in liver homogenates from four homozygote knockout mice (lanes 1–4), four heterozygote knockout (lanes 5–8), four wild-type (lanes 9–12) mice and purified human cathepsin L (std) using isoelectric focusing gel overlaid with the synthetic substrate, Z-Phe-Arg-NMec. (e) Analysis of cathepsin L, as panel d, except for the addition of the cathepsin B-specific inhibitor Ca074.

started as early as weaning and progressed rapidly to baldness by 8 weeks. Backcrossing onto a 129/Ola inbred background produced a phenotype identical to the original BL/6 × 129 homozygous cathepsin L mice.

Histological examination of skin of cathepsin L gene knockout mice

Histological examination of interscapular skin revealed differences between homozygote cathepsin L mice and the wild-type and heterozygote groups, which both showed normal skin structures (Figures 3 and 4). At 3 months, the skin of the BL/6 × 129 homozygotes displayed normal features, although hypotrichosis, characterized by few hair shafts, was observed in 25% of the homozygote animals (Figure 3b,c). Frequently, utricles (hair follicle expansions containing keratinized debris, located adjacent, and exterior, to the sebaceous glands) were observed in homozygote animals (Figure 3b).

Partially inbred cathepsin L mice (backcrossed for five generations to the inbred strain, BL6) showed slight epidermal thickening at 4 months (Figure 3d,e). There was a single example of a fully formed hair, orientated parallel to the plane of the

Figure 2 Comparison of the appearance of heterozygote (+/–) and homozygote (–/–) cathepsin L-deficient mice with wild-type (+/+) mice. For each group, the animal on the left is the homozygote. Heterozygote littermates are centrally positioned, and wild-type mice are on the right. (a) Three-month-old females, homozygotes display the characteristic phenotype detectable at weaning of reduced hair length and a reduction in density with hair of a dull greasy appearance; heterozygotes display a normal phenotype at this age. (b) Nine-month-old females, homozygotes display total alopecia; heterozygotes display pronounced partial hair loss. (c) Nine-month-old homozygote male knockouts exhibit baldness with patchy areas of sparse hair. Heterozygotes exhibit small areas of hair loss. All wild-type animals exhibited normal hair phenotype.

epidermis, lying within the dermis in a 4-month-old homozygote null mouse from the partially inbred colony (Figure 3d). This may have been the cause of some granulomatous inflammatory lesions seen in other animals, including 3-month-old homozygote animals from the B/L6×129 line. In a few instances, these lesions were elongated, lying within the dermis, and were orientated parallel to the skin surface (Figure 3c). Some homozygote cathepsin L mice from BL/6 backcrosses showed altered keratinization, resulting in plugs of keratin being found in the follicles (Figure 3e).

By 9 months, there was diffuse epidermal hyperplasia, with epidermal thickness increased to four to six cells as compared with the two- to three-cell thickness in wild-type mice (compare Figure 4a,b). The majority of these animals exhibited hypotrichosis. Homozygotes of both 3 and 9 months of age also exhibited a high incidence of severe hair shaft fragmentation (Figure 4c) when compared with wild-type mice. In addition, dermal or hypodermal granulomata were observed frequently at 9 months. These were characterized by chronic inflammation, occasionally with multinucleated giant cells centred upon a core of keratin, probably due to the abnormal orientation of hair follicles. A subacute folliculitis, occasionally accompanied by a subacute dermatitis, was also observed occasionally.

There was a striking difference in the spectrum of hair follicle differentiation in homozygote cathepsin L mice when compared with wild-type mice. In mammals, hair is produced in a cycle of tissue growth, degeneration and renewal, comprising three phases: during anagen, the follicle is reformed and a new hair is produced; catagen is characterized by cessation of hair elongation and hair follicle regression; whereas during telogen, the follicle is at rest. In homozygous mice aged 9 months, few anagen follicles were present and these appeared somewhat atrophic (Figure 4c). The remainder of the follicle population showed catagen or telogen phases. By contrast, in wild-type mice (Figures 3a and 4a), anagen and catagen stages of the hair follicle cycle were predominant with few telogen stages present.

Histomorphometric examination of bone of cathepsin L gene knockout mice

Gross analysis of femurs from cathepsin L heterozygote or homozygote mice *vs.* wild-type mice showed no significant difference in total bone ash mineral weight (Table 1). However, histomorphometric analysis demonstrated that the heterozygote and homozygote mice had a significant reduction in the amount of trabecular bone, although cortical bone volume was similar in all three genotypes.

Following ovariectomy, the removal of oestrogen drive resulted in a significant loss of bone, as determined by analysis using both ash weight and histomorphometry, in the wild-type, heterozygote and homozygote mice when compared with sham-operated animals. The extent of bone loss by ash weight was lowest in the homozygote cathepsin L mice and greatest in the wild-type mice, with intermediate bone loss in the heterozygote mice (Table 1).

The histomorphometric analysis demonstrated that the greatest bone loss in ovariectomized animals occurred in the metabolically active trabecular compartment, with bone volume decreasing by 51.7, 36.17 and 27.8% (compared with sham-operated animals) in the wild-type, heterozygote and homozygote animals, respectively (Table 1). A similar pattern of bone loss was also observed in the cortical bone,

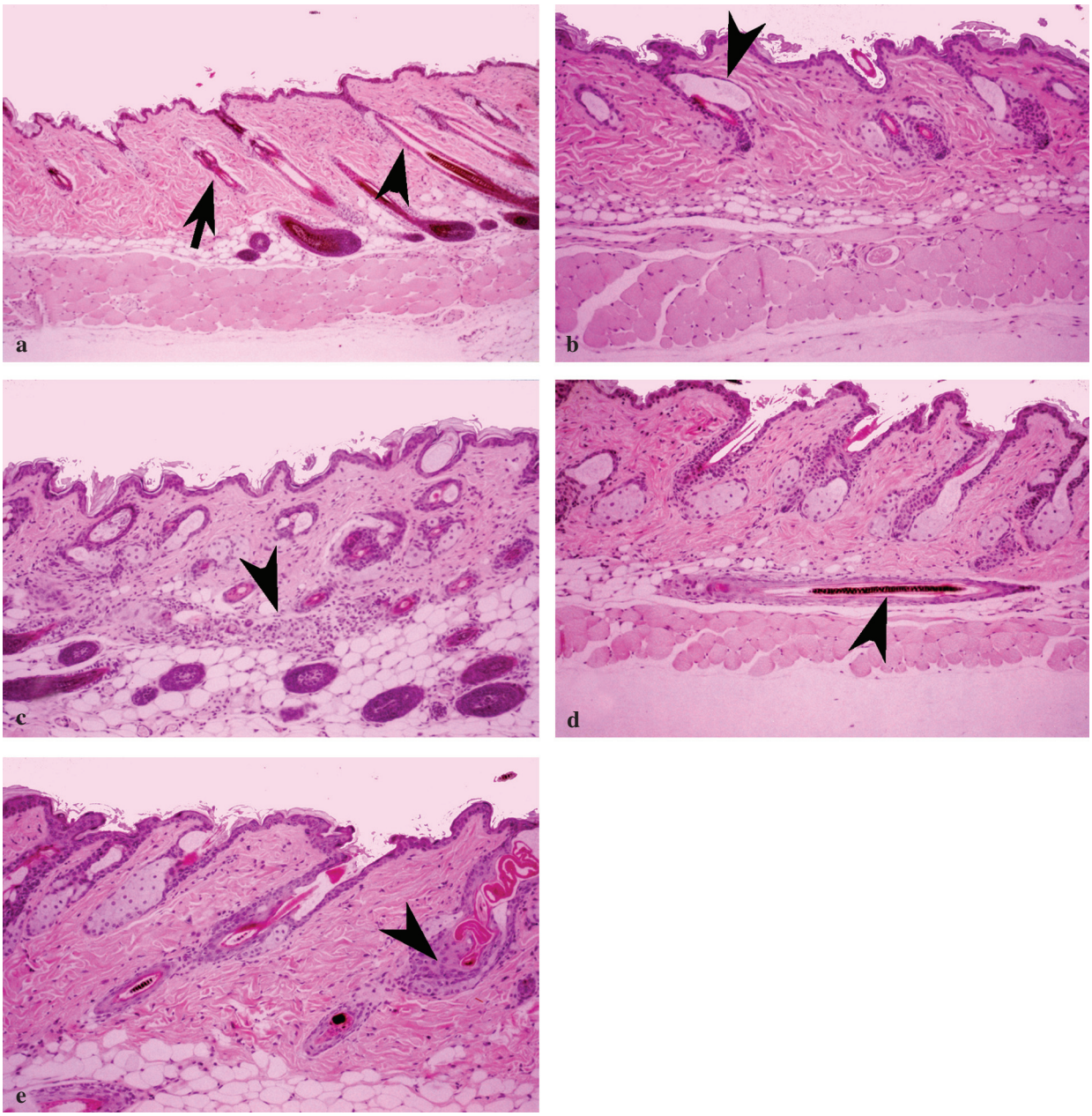

Figure 3 Histological analysis of skin from 3- and 4-month-old wild-type and cathepsin L homozygous mice. Panels a–c show skin sections from outbred mice. Panels d and e show skin sections from mice that have been backcrossed to BL/6 partners for five generations. (a) Skin section (×125) from a 3-month-old wild-type male of normal morphology. Note the apparent boundary between anagen (arrow) and catagen/telogen follicles (arrowhead). (b) Skin section (×250) from a 3-month-old homozygote cathepsin L male that has a normal epidermal thickness but showing utricles (arrowhead). (c) Skin section from a 3-month-old homozygote cathepsin L female showing hypodermal granulomatous inflammation with multinucleated giant cells centred on keratin (arrowhead) (×250). (d) Skin section from a 4-month-old homozygote cathepsin L male showing hypodermally located hair follicle (arrowhead) lying parallel to the plane of the skin (×250). (e) Skin section from a 4-month-old homozygote cathepsin L male. Note the normal epidermal thickness with abnormal follicular keratinization (arrowhead) (×250).

although, as expected, ovariectomy produced a smaller degree of loss in this, less metabolically active, bone compartment. There was no significant difference in either the femur ash weight or the cortical or trabecular bone volume in ovariectomized wild-type mice *vs.* the ovariectomized heterozygote or homozygote-deficient cathepsin L mice. However, analysis of

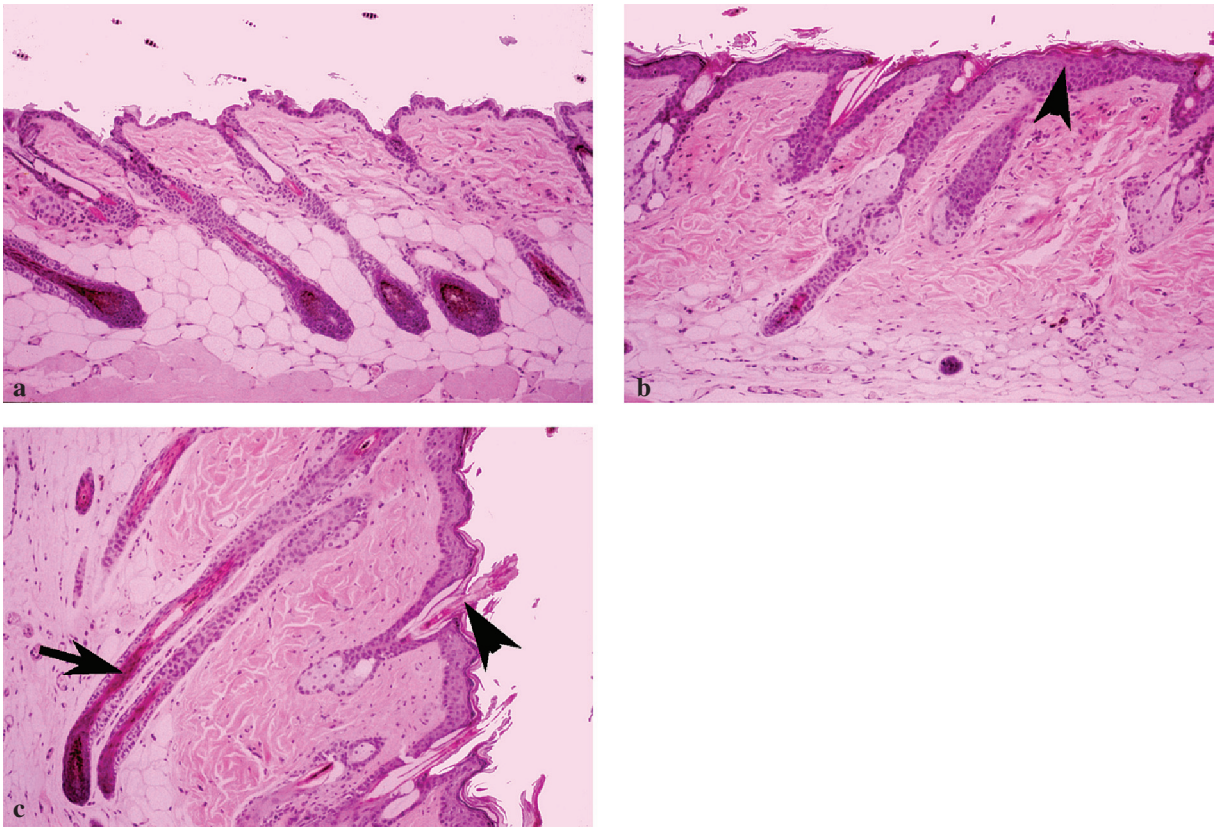

Figure 4 Histological analysis of skin from 9-month-old wild-type and outbred cathepsin L homozygous mice. (a) Skin section from a wild-type male showing a normal morphology (×250). (b) Skin section from a homozygous null male. Note the epidermal hyperplasia (thickening) extending into hair follicles (shown with a small arrowhead) (×250). (c) Skin section from a homozygote male. Epidermal hyperplasia, hair fragmentation (arrowhead), with anagen follicular atrophy (arrow) (×250).

Table 1 Effect of ovariectomy on the mineral and histomorphometric properties of bone in wild-type, cathepsin L heterozygote and homozygote mice

Parameter		Wild-type	*n*	Heterozygote	*n*	Homozygote	*n*
Femur ash weight	SHAM	31.2 mg	6	30.9 mg	7	29.7 mg	7
	Ovariectomy	25.9 mg ($P < 0.01$)	6	26.8 mg ($P < 0.05$)	4	26.5 mg ($P < 0.05$)	11
	Per cent bone loss after ovariectomy	16.98		13.26		10.77	
Cortical bone volume (relative units, mean ± SD)	SHAM	85.4 ± 3.1	6	84.8 ± 5.8	7	83.1 ± 4.9	7
	Ovariectomy	76.2 ± 4.0 ($P < 0.05$)	6	78.6 ± 6.1 (NS)	4	79.0 ± 5.3 (NS)	11
	Per cent bone loss after ovariectomy	10.77		7.31		4.93	
Trabecular bone volume (relative units, mean ± SD)	SHAM	14.3 ± 2.0	6	9.4 ± 1.7	7	7.9 ± 0.71	7
	Ovariectomy	6.9 ± 0.7 ($P < 0.01$)	6	6.0 ± 0.5 ($P < 0.05$)	4	5.7 ± 0.6 ($P < 0.01$)	11
	Per cent bone loss after ovariectomy	51.7		36.17		27.8	

Table 2 Histomorphometric analysis of osteoclast parameters associated with bone modelling (values represented as ±1 standard deviation)

Parameter/genotype	Wild-type ($n = 6$)	Heterozygotes ($n = 7$)	Homozygotes ($n = 7$)
Eroded surface/bone surface (%)	8.64 ± 0.81	7.47 ± 1.45	8.39 ± 1.38
Osteoclast surface/bone surface (%)	1.14 ± 0.22	0.96 ± 0.34	0.65 ± 0.27*
Osteoblast surface/bone surface (%)	10.15 ± 2.16	8.96 ± 3.04	7.99 ± 3.11
Erosion depth (μm)	10.18 ± 3.17	8.70 ± 3.56	5.44 ± 1.88*
Osteoclasts/mm of growth plate width	6.82 ± 2.77	5.53 ± 1.50	3.76 ± 0.98*

*Statistical significance ($P < 0.05$) between wild-type and homozygotes.

trabecular bone volume indicated a significant difference ($P < 0.01$) between wild-type sham-operated and wild-type homozygote animals. In addition, there was a significant difference ($P < 0.001$) between ovariectomized wild-type and ovariectomized homozygote animals, suggesting, independently of ovariectomy, lower trabecular bone volume in homozygote animals compared to wild-type controls.

At the cellular level, the most significant abnormalities were seen in osteoclast number and function. Within trabecular bone, in the homozygous group, the osteoclast number and eroded surfaces were both decreased (Table 2). The depth of erosion lacunae was also reduced and to a proportionately greater extent than the eroded surface parameters. These changes in osteoclast-related parameters were associated with an absolute decrease in osteoclast numbers, but the proportion of bone surfaces covered by osteoblasts was normal (Figure 5). There were no appreciable differences in the cortical bone in the three groups.

As there are no accepted histomorphometric criteria describing the matrix and cellular changes of the growth plate, we used the number of osteoclasts per unit area of the growth plate as an indicator of the functional integrity of bone resorption. Although the various chondrocyte zones of the growth plate were indistinguishable in the three groups, the osteoclastic remodelling of the mineralized cartilage differed considerably. In the heterozygote and homozygote animals, the general structure of the mineralized cartilage zone was disorganized as a consequence of abnormal osteoclastic remodelling. This altered growth plate osteoclasis resulted in the number of trabecular skeletons formed at the growth plates being less than in the normal controls. The number of these mineralized cartilaginous structures directly influences the number of trabeculae and the amount of trabecular bone as bone trabeculae are built on these structures. The reason for the decreased number of trabecular skeletons appeared to be the result of a decreased number of osteoclasts eroding the mineralized cartilage. Where trabecular skeletons were being formed, the proportion of surfaces on which osteoblastic bone deposition was occurring appeared normal.

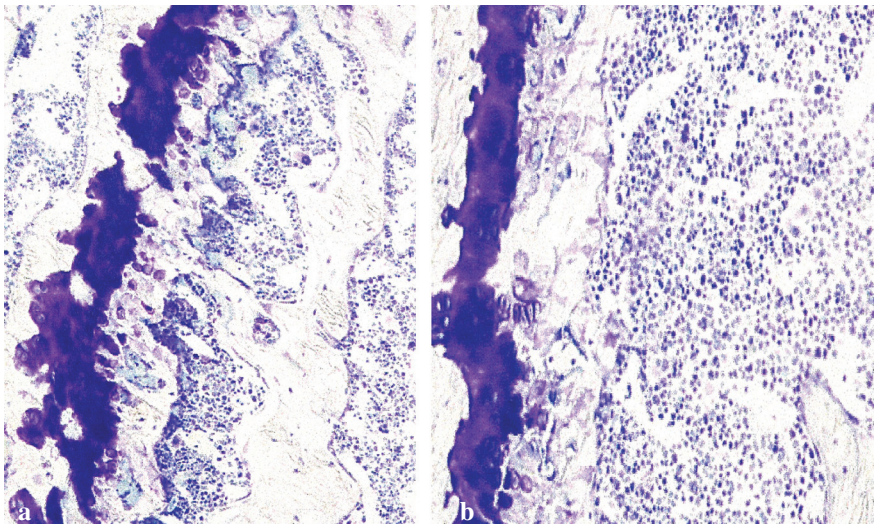

Figure 5 Histology of femoral bone from (a) wild-type mice and (b) homozygous cathepsin L knockout mice. In panel a, the growth plate is substantially thicker and more irregular in comparison with (b). This is consistent with the differences in osteoclast number between wild-type and homozygous cathepsin L knockout mouse bone (as indicated in Table 2) (toluidine blue stain: a, ×35; b, ×100).

Discussion

The results presented in this report demonstrate that a null mutation in the cathepsin L gene leads to abnormalities in skin and hair differentiation as well as alterations in bone structure and remodelling.

Cathepsin L homozygote mice exhibit epidermal hyperplasia, hair shaft fragmentation, utricle formation and gradual hair loss leading to extensive baldness. This was more pronounced in female when compared with male mice. These features share some similarity to the rodent models of alopecia areata, where, in DEBR rats and C3H/HeJ mice, females displayed greater hair loss, more rapidly and to a greater extent, than males (McElwee *et al*. 1998). Backcrossing the cathepsin L null gene to BL/6 mice revealed a more pronounced phenotype, with hair loss starting at weaning and progressing to baldness by 8 weeks. This may indicate that the genetic background of the resulting mice had an influence on the resulting phenotype.

Roth *et al*. (2000) described histopathological changes in the skin of cathepsin L-deficient mice that resemble closely those seen in the spontaneous mouse mutant *furless* and which were present in the mice studied in our investigations. It is striking that both the histological alterations in differentiation of hair follicles and in increased thickness of the epidermis and their timing were observed in independent studies by Roth *et al*. (2000) and ourselves.

These observations provide evidence of significant alterations in epithelial growth and tissue differentiation in skin associated with cathepsin L disruption. It has been postulated that cathepsin L may partly regulate both protein breakdown and intracellular protein metabolism during the course of cell differentiation, and terminal differentiation, in cultured rat keratinocytes (Tanabe *et al*. 1991). Cathepsin L-like proteinase has been purified from rat epidermis (Harvima *et al*. 1987), and inactive precursors of cathepsin L have been identified in normal human epidermis. Activated cathepsin L has been linked to the pathology of psoriasis (Kawada *et al*. 1978). Additionally, a cathepsin L-like proteinase has been shown to play a role in processing filaggrin in the epidermis (Kawada *et al*. 1995). These intermediate filament-associated proteins are processed during differentiation of the skin, suggesting that cathepsin L-like proteinases may be implicated in skin differentiation. However, although the homozygous cathepsin L mice described here displayed epidermal hyperplasia, which is associated with psoriasis, they did not show significant inflammation of the skin. A transgenic model of psoriasis has been produced, where integrin subunits are expressed in the suprabasal epidermal layers: These mice exhibit epidermal hyperplasia, abnormal keratinocyte differentiation and inflammation of the skin (Carroll *et al*. 1995), in contrast to the mice described in this report.

There are several other examples of transgenic and gene knockout models of hair loss and skin differentiation. Transgenic mice containing a human BMP-4 cDNA under the control of the bovine cytokeratin IV promoter displayed deficiencies in hair growth, resulting in progressive balding and whisker defects, similar to the effects observed in cathepsin L knockout mice. However, the BMP-4 transgenic mice showed cessation of cell proliferation, in contrast to the observations in the cathepsin L knockout mice (Blessing *et al*. 1993). Transgenic mice expressing transforming growth factor-α (TGF-α) in the stratified squamous epithelia showed epidermal hyperplasia, also seen in the cathepsin L null mice, implicating TGF-α as a contributory mediator of epidermal thickness during development and differentiation (Vassar & Fuchs 1991). In the present study, there was an example of a follicle containing a fully formed hair, growing horizontally in the hypodermal adipose tissue in a homozygous mouse. TGF-α-deficient mice also showed this feature but at a higher frequency (Luetteke *et al*. 1993). However, unlike these mice, cathepsin L null mice failed to show wavy hair and eyelid defects. Interestingly, dermal granulomata were observed frequently in outbred cathepsin L homozygous mice at 9 months. It is possible that this phenomenon is due to inflammatory processes associated with abnormal hair follicle orientation, retention and trapping within dermal or hypodermal locations.

It has been proposed that cathepsin L may modulate the levels of proteins involved in signal transduction. Hiwasa *et al*. (1988) reported that epidermal growth factor receptors (EGFRs) are cleaved by a cathepsin L-like protease. EGFR signalling plays an important role in hair follicle and skin development, and mutant mice lacking EGFR have whisker and skin defects, including a thinner epidermis and abnormal epidermal organization (Sibilia & Wagner 1995). These data, together with the findings reported here, suggest that cathepsin L may play a significant role in modulating signal transduction proteins involved in skin differentiation.

Cathepsins K and L have been postulated to play a role in bone remodelling due to their ability to degrade bone matrix proteins, predominantly type I collagen (Kirschke *et al*. 1982). Data from the cathepsin K knockout mouse support this role, as mice displayed an osteopetrotic phenotype with excessive trabeculation of the bone-marrow space (Saftig *et al*. 1998, 2000). In this study, cathepsin L knockouts exhibited a different phenotype in which there was a decrease in trabecular bone volume. This effect was greater in the homozygote than the heterozygote cathepsin L mice. Reduced bone mass may suggest that cathepsin L is involved in endochondrial ossification, a hypothesis that is supported by cathepsin L-induced cleavage of cartilage matrix proteins (Maciewicz *et al*. 1990), thereby resulting in reabsorption of the cartilaginous matrix, allowing angiogenesis and new bone formation. In addition, recent *in situ* hybridization

indicated that in mouse long bone, cathepsin K mRNAs were predominantly observed in multinucleated chondroclastic and osteoclastic cells at the osteochondral junction, whilst cathepsin L was localized to osteoclasts and hypertrophic and proliferating chondrocytes (Soderstrom *et al*. 1999). Similar results were observed in human tissue, where both cathepsin L and cathepsin K were immunolocalized to osteoclasts and chondroclasts attached to bone and cartilage matrix, respectively, but only cathepsin L was found in proliferating and hypertrophic chondrocytes (Nakase *et al*. 2000). The observation that cathepsin L but not cathepsin K localizes to hypertrophic chondrocytes provides a rational explanation for the opposing effects on bone that these two knockout mice exhibit.

Further work supports the hypothesis that these two proteinases have distinct roles in bone formation and remodelling. Furuyama & Fujisawa (2000a) have shown, using antisense to cathepsins K and L, that in mouse calvarial bone cultures, cathepsin K is constitutively synthesized and is the predominant collagenolytic cysteine proteinase. However, cathepsin L activity in osteoclasts is upregulated by stimulants of bone resorption including parathyroid hormone, interleukin-1α (IL-1α), IL-6 or tumour necrosis factor-α (TNF-α), and the enzyme then acts with cathepsin K to degrade type I collagen.

Our study has shown that wild-type, heterozygote and homozygote cathepsin L mice lost bone after removal of endogenous oestrogen (ovariectomy) with the absolute amount of bone loss being lowest in the homozygote group. In wild-type mice, bone was lost from both the cortical and trabecular bone. In contrast, heterozygote and homozygote cathepsin L mice had a markedly reduced loss of trabecular when compared with cortical bone. This may suggest that cathepsin L has a role in the remodelling of trabecular bone in response to metabolic and, possibly, environmental stimuli. As trabecular bone loss is important in diseases such as osteoporosis, these data suggest that cathepsin L may have a role in this disease. This hypothesis is supported by recent data that indicate that both cathepsin K and cathepsin L are involved in *in vivo* bone remodelling in an animal model of osteoporosis (Furuyama & Fujisawa 2000b). Here, the activity of both cathepsin K and cathepsin L in mouse calvaria indicated a significant increase in activity in ovariectomized animals *vs*. sham-operated animals. This activity was reduced in the presence of estradiol-16β.

The cellular abnormalities leading to a reduced trabecular bone mass were decreased osteoclastic activity at the growth plate where trabeculae are formed. Osteoclastic activity in the trabecular bone was also reduced and was made up of a moderate decrease in cell number and a marked decrease in the activity of individual cells. In this study, the animals were not given a label marker of bone formation, such as two doses of tetracycline, but as far as can be assessed from static (as opposed to dynamic) parameters, osteoblastic activity is normal.

The histomorphometric parameters utilized in our studies contribute to our understanding of why the common cellular abnormality of decreased osteoclastic activity could lead to a decrease in trabecular bone volume in whole heterozygote and homozygote animals and the apparently paradoxical effect of a diminished osteoclastic response to ovariectomy.

In summary, disruption of the cathepsin L gene leads to major abnormalities in skin and hair development and differentiation and alterations in trabecular bone deposition and reduces the response of bone to oestrogen withdrawal. These observations suggest that the control of cathepsin L expression or regulation of its activity may have therapeutic applications for the treatment of hyperproliferative skin disorders and in bone remodelling diseases such as osteoporosis.

Acknowledgements

The authors are grateful to the Histology Group and Safety Assessment for their contributions to these studies. We thank David Melton for providing HM-1 ES cells.

References

Adra C.N., Boer P.H., McBurney M.W. (1987) Cloning and expression of the mouse pgk-1 gene and the nucleotide sequence of its promoter. *Gene* **60**, 65–75.

Blessing M., Nanney L.B., King L.E., Jones C.M., Hogan B.L.M. (1993) Transgenic mice as a model to study the role of TGF-beta-related modules in hair follicles. *Genes Dev.* **7**, 204–215.

Carroll J.M., Romero R., Watt F.M. (1995) Suprabasal integrin expression in the epidermis of transgenic mice results in developmental defects and a phenotype resembling psoriasis. *Cell* **83**, 957–968.

Deussing J., Roth W., Saftig P., Peters C., Ploegh H., Villadangos J.A. (1998) Cathepsins B and D are dispensable for major histocompatibility complex class II-mediated antigen presentation. *Proc. Natl. Acad. Sci. USA* **95**, 4516–4521.

Everts V., van der Zee E., Creemers L., Beertsen W. (1996) Phagocytosis and intracellular digestion of collagen, its role in turnover and remodelling. *Histochem. J.* **28**, 229–245.

Furuyama N., Fujisawa Y. (2000a) Distinct roles of cathepsin K and cathepsin L in osteoclastic bone resorption. *Endocr. Res.* **26**, 189–204.

Furuyama N., Fujisawa Y. (2000b) Regulation of collagenolytic cysteine protease synthesis by estrogen in osteoclasts. *Steroids* **65**, 371–378.

Halangk W., Lerch M.M., Brandt-Nedelev B., Roth W., Ruthenbuerger M. (2000) Role of cathepsin B in intracellular

trypsinogen activation and the onset of acute pancreatitis. *J. Clin. Invest.* **106**, 773–781.

Harvima R.J., Yabe K., Fraki J.E., Fukuyama K., Epstein W.L. (1987) Separation and identification of cathepsins in newborn rat epidermis. *J. Invest. Dermatol.* **88**, 393–397.

Haworth C.S., Webb K.A., Egan J.J. *et al.* (2000) Bone histomorphometry in adult patients with cystic fibrosis. *Chest* **118**, 434–439.

Hiwasa T., Sakiyama S., Yokoyama S. *et al.* (1988) Degradation of epidermal growth factor receptors by cathepsin 1-like protease: Inhibition of the degradation by c-Ha-ras gene products. *FEBS Lett.* **233**, 367–370.

Katunuma N., Matsunaga Y., Matsui A. *et al.* (1998) Novel physiological functions of cathepsins B and L on antigen processing and osteoclastic bone resorption. *Adv. Enzyme Regul.* **38**, 235–251.

Kawada A., Hara K., Hirums M., Noguchi H., Ishibashi A. (1995) Rat epidermal cathepsin 1-like proteinase: Purification and some hydrolytic properties toward filaggrin and synthetic substrates. *J. Biochem.* **118**, 332–337.

Kawada A., Hara K., Kominami E., Hiruma M., Noguchi H., Ishibashi A. (1978) Processing of cathepsins L, B and D in psoriatic epidermis. *Arch. Dermatol. Res.* **289**, 87–93.

Kirschke H., Kembhavi A.A., Bohley P., Barrett A.J. (1982) Action of rat liver cathepsin L on collagen and other substrates. *Biochem. J.* **201**, 367–372.

Laird P.W., Zijderveld A., Linders K., Rudnicki M.A., Jaenisch R., Berns A. (1991) Simplified mammalian DNA isolation procedure. *Nucleic Acids Res.* **19**, 4293.

Lalor B.C., France M.W., Powell D., Adams P.H., Counihan T.B. (1986) Bone and mineral metabolism in chronic alcohol abuse. *Q. J. Med.* **59**, 497–511.

Luetteke N.C., Qiu T.H., Peiffer R.L., Smithies O.P., Lee D.C. (1993) TF deficiency results in hair follicle and eye abnormalities in targeted and waved-1 mice. *Cell* **73**, 263–278.

Maciewicz R.A., Etherington D.J. (1988) A comparison of four cathepsins (B, L, N and S) with collagenolytic activity from rabbit spleen. *Biochem. J.* **256**, 433–440.

Maciewicz R.A., Wardale R.J., Etherington D.J., Paraskeva C. (1989) Immunodetection of cathepsins B and L present in and secreted from pre-malignant and malignant colorectal tumour cell lines. *Int. J. Cancer* **43**, 478–486.

Maciewicz R.A., Wotton S.F., Etherington D.J., Duance V.C. (1990) Susceptibility of the cartilage collagens types II, IX and XI to degradation by the cysteine proteinases, cathepsins B and L. *FEBS Lett.* **269**, 189–193.

McElwee K.J., Boggess D., Olivry T. *et al.* (1998) Comparison of alopecia areata in human and nonhuman mammalian species. *Pathobiology* **66**, 90–107.

McPheat J.C., Potts W.J., Miller C.C.J. (1991) A simple, efficient and rapid method for isolating embryonic stem cell clones for analysis in gene targeting experiments. *Methods Mol. Cell. Biol.* **2**, 289–291.

Nakagawa T.Y., Brissette W.H., Lira P.D., Griffiths R.J., Petrushova N. (1999) Impaired invariant chain degradation and antigen presentation and diminished collagen-induced arthritis in cathepsin S null mice. *Immunity* **10**, 207–217.

Nakagawa T., Roth W., Wong P. *et al.* (1998) Cathepsin L: critical role in Ii degradation and CD4 T cell selection in the thymus. *Science* **280**, 450–453.

Nakase T., Kaneko M., Tomita T. *et al.* (2000) Immunohistochemical detection of cathepsin D, K, and L in the process of endochondral ossification in the human. *Histochem. Cell Biol.* **114**, 21–27.

Parfitt A.M., Drezner M.K., Glorieux F.H. (1987) Bone histomorphometry: standardization of nomenclature, symbols and units. Report of the ASBMR Histomorphometry Nomenclature Committee. *J. Bone Miner. Res.* **2**, 595–610.

Roth W., Deussing J., Botchkarev V.A. *et al.* (2000) Cathepsin L deficiency as molecular defect of *furless*: hyperproliferation of keratinocytes and pertubation of hair follicle cycling. *FASEB J.* **14**, 2075–2086.

Saftig P., Hunziker E., Everts V. *et al.* (2000) Functions of cathepsin K in bone resorption. Lessons from cathepsin K deficient mice. *Adv. Exp. Med. Biol.* **477**, 293–303.

Saftig P., Hunziker E., Wehmeyer O. *et al.* (1998) Impaired osteoclastic bone resorption leads to osteopetrosis in cathepsin-K-deficient mice. *Proc. Natl. Acad. Sci. USA* **95**, 13453–13458.

Shi G.-P., Bryant R., Riese R., Verhelst S., Driessen C. (2000) Role for cathepsin F in invariant chain processing and major histocompatibility complex class II peptide loading by macrophages. *J. Exp. Med.* **191**, 1177–1186.

Shi G.P., Villadangos J.A., Dranoff G. *et al.* (1999) Cathepsin S required for normal MHC class II peptide loading and germinal center development. *Immunity* **10**, 197–206.

Sibilia M., Wagner E. (1995) Strain-dependent epithelial defects in mice lacking the EGF receptor. *Science* **269**, 234–237.

Soderstrom M., Salminen H., Glumoff V., Kirschke H., Aro H., Vuorio E. (1999) Cathepsin expression during skeletal development. *Biochim. Biophys. Acta* **1446**, 35–46.

Tanabe H., Kumagai N., Tsukahara T. *et al.* (1991) Changes of lysosomal proteinase activities and their expression in rat cultured keratinocytes during differentiation. *Biochim. Biophys. Acta* **1094**, 281–287.

Tybulewicz V.L.J., Crawford C.E., Jackson P.K., Bronson R.T., Mulligan R.C. (1991) Neonatal lethality and lymphopenia in mice with a homozygous disruption of the C-abl proto-oncogene. *Cell* **65**, 1153–1163.

Vassar R., Fuchs E. (1991) Transgenic mice provide new insights into the role of TGF-alpha during epidermal development and differentiation. *Genes Dev.* **5**, 714–727.